Chem Soc Rev

This article was published as part of the

2008 Chemistry at Surfaces issue

Reviewing the latest developments in surface science

All authors contributed to this issue in honour of the 2007 Nobel Prize winner Professor Gerhard Ertl

Please take a look at the issue 10 table of contents to access the other reviews

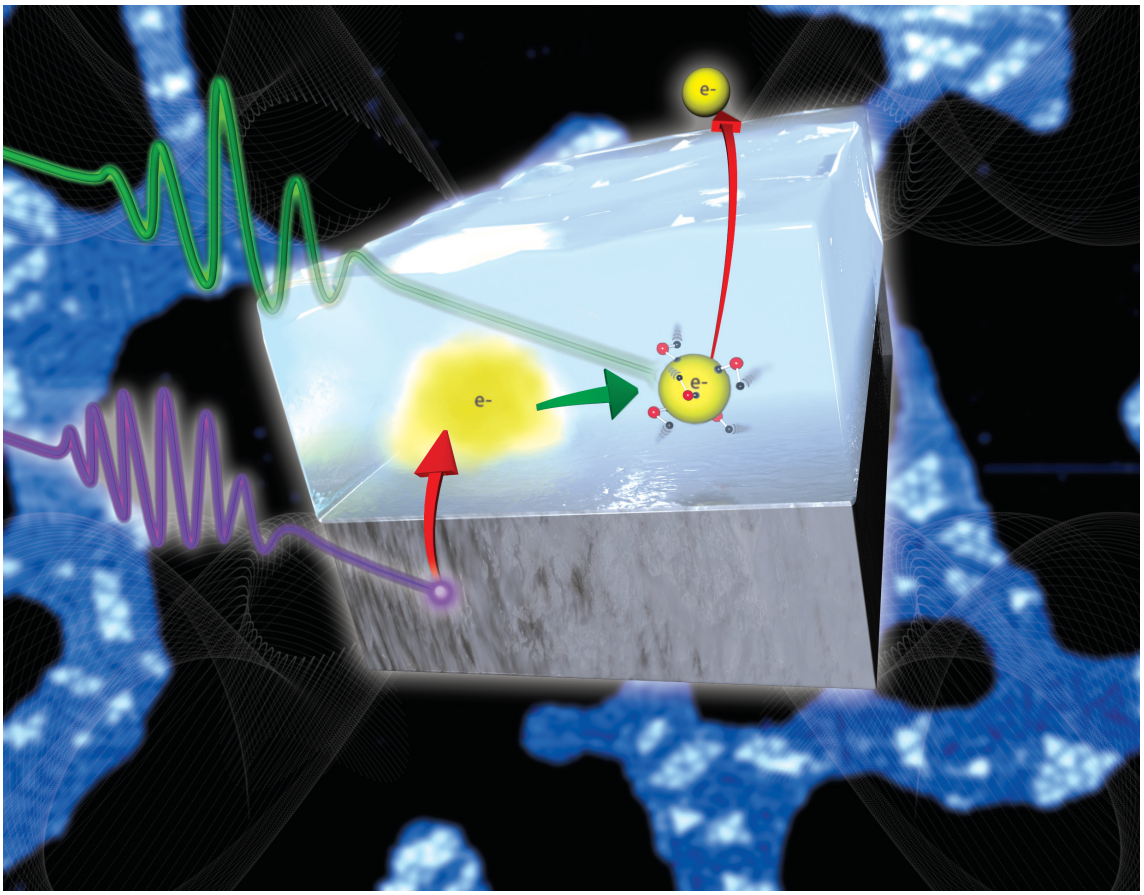

Automotive catalysis studied by surface science†

Michael Bowker

Received 24th April 2008
First published as an Advance Article on the web 5th August 2008
DOI: 10.1039/b719206c

In this *tutorial review* I discuss the significant impact that surface science has had on our understanding of the catalytic phenomena associated with automobile exhaust depollution catalysis. For oxidation reactions it has generally been found that reactions are self-poisoned at low temperatures by the presence of strongly adsorbed reactants (such as molecular CO and NO), and that the rapid acceleration in rate at elevated temperatures (often called 'light-off') is due to the desorption of such adsorbates, which then frees up sites for dissociation and hence for oxidation reactions. In some circumstances such autocatalytic phenomena can then manifest themselves as oscillatory reactions which can vary in rate in both space and time. For NO reduction, the efficiency of depollution (by production of molecular nitrogen) is strongly affected by the nature of the metal used. Rh is extremely effective because it can dissociate NO much more readily than metals such as Pd and Pt, enabling oxygen removal (by reaction with CO to CO_2) even at room temperature. Rh is also very selective in producing predominantly N_2, rather than N_2O. NO_x storage and reduction (NSR) is an important recent development for removal of NO_x under the highly oxidising conditions of a lean-burn engine exhaust, and the strategy involves storing NO_x on BaO under oxidising conditions followed by the creation of reducing conditions to de-store and reduce it to nitrogen. By the use of STM it has been shown that this storage process is extremely facile, occurring fast even under UHV conditions, and that the storage occurs on BaO in the vicinity of Pt, with most of the oxide being converted to nitrate.

1 Automotive catalysis

Since legislation was initiated in California in the early 1970s,[1,2] it has extended both globally and in terms of the severity of the requirements for the removal of pollutants from the exhausts of automobiles. At first catalytic amelioration was simply related to reducing CO and hydrocarbon emissions, achieved with relatively straightforward oxidation catalysts such as Pt/alumina.[1,2] The next stage was to include NO_x emissions in the legislation and to tighten the limits for CO and hydrocarbon emissions. This involved catalyst development in several respects. Firstly, oxygen storage components were required in order to enhance CO and hydrocarbon conversion during the rich part of the engine cycle, and secondly NO_x conversion was required, which was achieved at that time by the incorporation of Rh in such catalysts.[1–4] Rh is particularly effective for NO_x reduction reactions with CO or H_2. Most of this technology was applied to normally-aspirated petrol engines, where the air : fuel ratio is kept close to stoichiometric, that is around neutral in terms of oxidising or reducing power of the exhaust. More recently fuel efficiency has come to the fore in internal combustion engines and so both lean-burn petrol and diesel engines have increased their market penetration. These both present new problems because such lean-burn engines result in a net oxygen-rich exhaust gas. It then becomes extremely difficult to reduce NO_x emissions by conversion to benign N_2. Toyota presented a very clever solution to this problem in the early 1990s,[5–7] which consisted of adding a NO_x storage medium (usually a Ba salt) to the washcoat catalyst. This stored the unconverted NO_x (essentially due to the net conversion of BaO to $Ba(NO_3)_2$) during the lean operation. An integral part of this innovation was to operate the engine in a fuel-rich mode periodically for a short period of time, producing a reducing gas consisting of CO and H_2, among other compounds. These then react with the barium nitrate, forming N_2, CO_2 and H_2O, and regenerating the initial Ba salt. Effectively the fuel acts as a reductant and to convert the nitrate back to oxide and NO_x, the NO_x being reduced to N_2 over the now-reduced precious metal component(s). Reviews of such catalysis have appeared recently.[8,9]

Wolfson Nanoscience Laboratory, School of Chemistry, Cardiff University, Cardiff, UK CF10 3AT. E-mail: bowkerm@cf.ac.uk
† Part of a thematic issue covering reactions at surfaces in honour of the 2007 Nobel Prize winner Professor Gerhard Ertl.

Michael Bowker

Michael Bowker is Director of the Wolfson Nanoscience Laboratory in the School of Chemistry at Cardiff University and heads the Heterogeneous Catalysis and Surface Science Group. His research covers the fields of nanoscience, surface science and catalysis. He has previously worked in academic (Stanford, Liverpool and Reading Universities) and industrial (ICIplc) positions.

Most of the reaction events involved in these processes occur at the surface, and therefore the surface science approach has been, and continues to be, an important way to obtain a detailed understanding of these phenomena. In what follows we will outline some of the developments that have occurred in this field over the past thirty years or so. The work in surface science in this area has, to a degree, stemmed from the developments in the catalysis and so in what follows we will outline developments in the three main phases mentioned above, that is, simple oxidation (highlighted by the CO oxidation reaction), NO_x removal and then NSR.

2 Catalytic oxidation—the $CO–O_2$ reaction

Ertl was one of the first to study the simplest of these automobile-exhaust treatment reactions (CO oxidation) using the methods of surface science, and published a number of elegant and seminal papers in the 1970s using mainly molecular beam methods to understand more about the kinetics and mechanism of the reaction.[10–14] One of the important aspects of this is one which is generally important in the field and can be illustrated by Fig. 1a.[15] Here it can be seen that there is a maximum in reaction rate with increasing temperature and that there is a relatively sharp increase in rate at the onset of reaction. This increase is related to the so-called 'light-off' phenomenon in exhaust catalysis where there is also a sudden increase in rate. An example of real data from Engel and Ertl[10] is given in Fig. 1b, showing the same general form, with the onset for one set of data being at ~470 K. This behaviour can be explained in the following way. As stated by Engel and Ertl,[14] these reactions are of the Langmuir–Hinshelwood (LH) type,[15,16] with no evidence for Eley–Rideal (ER) reactions. By definition, LH reactions occur between relatively strongly adsorbed species, bound to the surface of the catalyst, whereas ER reactions occur by direct reaction between one surface species and a colliding gas phase molecule. The simplest form of the Langmuir–Hinshelwood equation is:

$$\text{Rate}_{CO_2} = k\theta_{CO}\theta_O \qquad (1)$$

where k is the rate constant for the surface reaction and θ is the coverage of each adsorbed species, molecular CO and atomic oxygen in this case.

The explanation for the 'light-off' described above is that it is an autocatalytic phenomenon. This is illustrated particularly nicely by the time-resolved XPS data of Fig. 2.[17,18] These show stacked XPS spectra (as closely packed horizontal lines, with intensity represented by colour variation). Here it can seen that as the sample is heated in the presence of gas phase CO and oxygen, CO dominates the surface at low temperature, with no dissociated oxygen (binding energy ~530 eV), but that there is a sudden change at ~400 K. At that point there is a switch in surface coverage from adsorbed CO to mainly adsorbed atomic oxygen; this is the point of light-off (Fig. 2 and 3 at ~360 K). Fig. 3 also shows the coverage values determined from the XPS as a function of temperature to illustrate these points further. The surface is dominated by CO at low temperature (Fig. 3, ●), but it begins to desorb at ~350 K, and at that point oxygen can begin to dissociate,

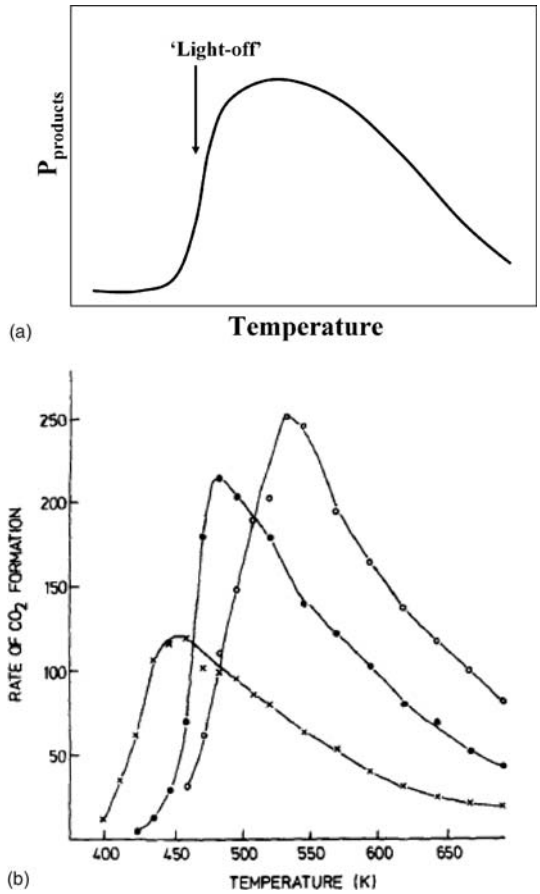

Fig. 1 (a) Schematic diagram of the light-off phenomenon in catalysis. (b) A specific example from the work of Engel and Ertl.[14] The curves are for reaction of an oxygen molecular beam with background CO on Pd(111), for three different background CO pressures. In order of increasing rate the three CO pressures were 1×10^{-7}, 3×10^{-7}, 1×10^{-6} torr, with a fixed oxygen pressure of 4×10^{-7} torr.

inducing a further reduction in CO coverage by reaction, so that oxygen dominates the surface above 400 K (Fig. 3, ○) where the lifetime of CO is relatively short. The combined surface coverage by adsorbed CO and oxygen atoms is always high (Fig. 3, □) during these changes. Since the catalyst surface is essentially poisoned by adsorbed CO at the low temperature end of these curves, then the overall surface reaction can be written as follows:

$$2CO_a + O_{2g} + 2S \rightarrow 2CO_{2g} + 4S \qquad (2)$$

This results from a combination of elementary reactions, as follows:

$$O_{2g} + 2S \rightarrow 2O_a$$

$$2CO_a + 2O_a \rightarrow 2CO_{2g} + 4S$$

On the left hand side of eqn (2) we show gas phase molecular oxygen adsorbing on a surface with adsorbed CO present, as is the situation before light-off. It requires two free sites (S) to be available for oxygen to dissociate and, since once the oxygen dissociates the reaction is fast, CO_2 is quickly produced and, in so doing, produces four free sites. Thus a reactant (site S) is

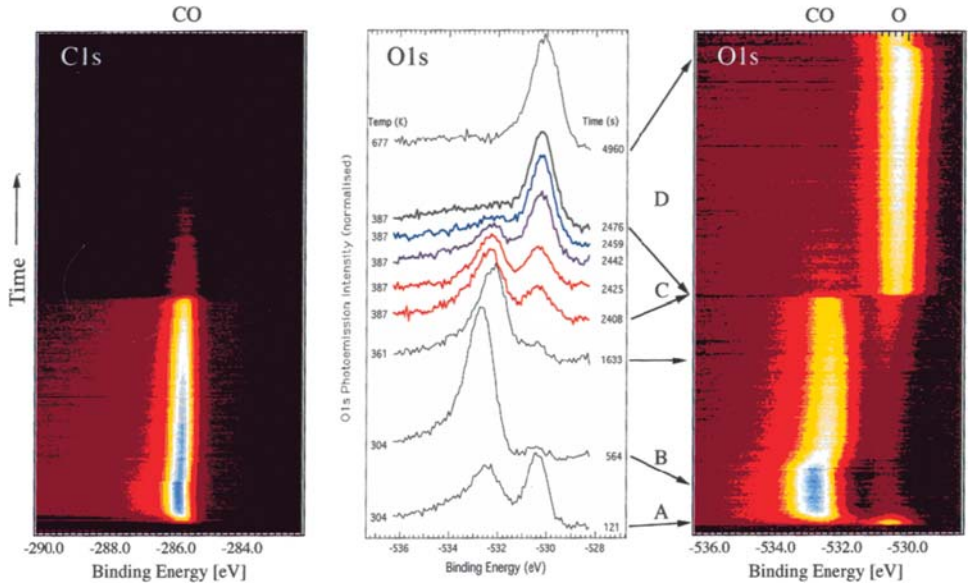

Fig. 2 Temperature-programmed XPS experiments, showing the abruptness of the light-off phenomenon very clearly. In the left and right panels are shown the XPS intensity (in terms of colour, light being high intensity, dark being low) as the surface is heated in the presence of CO and oxygen gas. The peaks at 286 and ~533 eV are due to adsorbed molecular CO, while that at 530 eV is due to atomic oxygen. In the centre panel detailed XPS spectra in the O(1s) region are shown, representing the various phases of surface composition during the experiment. In that panel the numbers on the right represent the time in seconds since the start of exposure to CO and oxygen, while on the left is the temperature of the surface. Note the change in surface coverage under near isothermal conditions in region C, indicative of an autocatalytic reaction.

produced in excess on the right hand side and so the reaction becomes self-accelerating. Such a positive feedback process is an essential part of the kinetic oscillations described in great detail by Ertl in later publications[19–24] and cited in the Nobel Prize award.[25]

Note that in Fig. 3 the product of the CO and O coverages (▲) follows the shape of the rate curve for CO_2 production determined in other measurements. Thus it is clear that in terms of the Langmuir equation above (eqn (1)), the product of the coverages dominates the shape of the light-off curve and not the surface reaction rate constant, which increases exponentially with temperature. An excellent review of the temperature and pressure dependence of CO oxidation on single crystal precious metals has been presented by Santra and Goodman.[26]

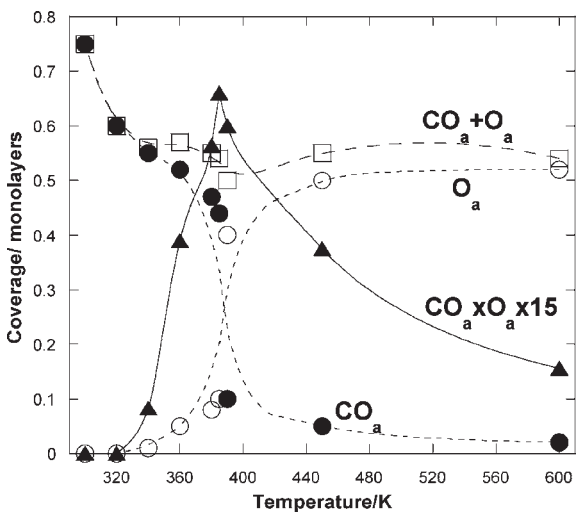

Fig. 3 Changes in surface coverage of CO (●) and atomic oxygen (○) as a function of temperature, derived from the XPS measurements. Also shown is the sum of the coverages (□), the total coverage always being at least 0.5 monolayers and the product of the coverages (▲), which relates to the Langmuir–Hinshelwood mechanism (eqn (1) in the text). The major transition in coverage occurs at 390 K.

When using high area catalysts under ambient conditions, this light-off is usually even more noticeable, because the reactions are exothermic and so there is a further feedback process of heating to enhance the rate even more (and sometimes resulting in so much heat release that the catalyst glows, hence the term 'light-off'). It is well-known that the CO desorption peak in TPD from group 10 metals is at ~450 K, and that desorption starts earlier,[27] which correlates well with the beginnings of light-off shown above. Due to the presence of high pressures of CO in the exhaust, the coverage only drops low enough to allow O_2 adsorption at somewhat higher temperatures in the real exhaust situation than on single crystals at low pressure. It is interesting to note that Au shows the ability to oxidise CO at much lower temperatures, even as low as 230 K,[28–31] at least partly due to the fact that CO is bound much more weakly on gold and therefore it is not so easily self-poisoned.

Relating to the feedback mechanism, Ertl[23–25] and others[32,33] have spent considerable effort on studying the effects on reaction kinetics, hence why Ertl's Nobel Prize citation includes "*for groundbreaking studies in surface chemistry*" and "*for his thorough studies of fundamental molecular processes at the gas–solid interface*".[25] One of the most remarkable of these is the ability of the reaction, under the correct (and usually very narrowly defined) conditions

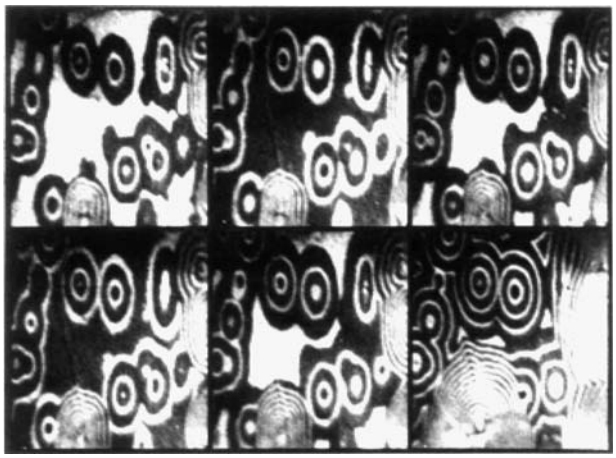

Fig. 4 PEEM experiments showing oscillations in time and space of the CO oxidation reaction on Pt(110) at a surface temperature of 427 K.[21] The image sizes are 0.2 × 0.3 mm, with pressures of CO of 3×10^{-5} mbar and oxygen 3×10^{-4} mbar. The time intervals between images is 4.1 s, except for the last two it is 30 s. The contrast seen reflects areas of high CO coverage (bright) and high atomic oxygen coverage (dark), which also reflects the differing work functions for the two adsorbates.

(temperature, pressure, CO : O_2 ratio) to become unstable and to go into periodic oscillations, either in a regular manner, or in a chaotic manner. In turn this can also be spatially periodic, reminiscent of older discoveries such as the Belousov–Zhabotinskii reaction in which malonic acid is oxidised in aqueous solution.[34] Ertl used PEEM (photoelectron electron microscopy) to image these types of oscillations on various surfaces with the startling results of the type shown in Fig. 4.[21] Here there is spatial and temporal variation of the contrasting regions, the contrast being due to areas of differing surface concentrations of CO. In the case of Fig. 4, light areas are regions of adsorbed CO, whereas dark areas comprise adsorbed oxygen atoms. The differences are measured by the electron emission from these areas, which relates to the work function, and in turn again relates to the coverage of CO and oxygen.[23,24]

3 NO_x conversion and the CO–NO reaction: why Rh is so effective

Similar considerations to the above simple reaction apply to the CO–NO reaction, but there are some important differences:

(i) The NO molecular bond is stronger than that in O_2.

(ii) The molecular states of NO are much more strongly bound than are those of molecular oxygen.

(iii) It is a hetero-atomic molecule.

These facts have important consequences for the reaction. Relating to (i) it is more difficult to dissociate the NO bond than the O_2 bond (gas phase bond dissociation energies are 630 kJ mol^{-1} and 500 kJ mol^{-1}, respectively). In relation to precious metal adsorption, then, it is recognised that it is much easier to dissociate NO on Rh than it is on Pt and Pd. As a consequence of (ii) there may be competition between molecular and dissociative NO adsorption states, which does not occur for oxygen under exhaust conditions, and item (iii) above leads to the possibility of more reaction products. In particular, we might produce N_2 and N_2O, and possibly even NO_2 as reaction products, depending on the exact conditions.[35,36] Fig. 5 clearly shows the differences between Rh and Pd for the CO–NO reaction. Rh dissociates NO at ambient temperature,[35] as a result of which CO_2 is produced upon subsequent CO exposure, whereas Pd does not dissociate NO under these conditions and no CO_2 is produced.[36,37] It is notable, however that for Pd both CO and NO adsorb on the surface very efficiently (sticking probabilities are 0.5 and 0.4, respectively), but that CO is displaced from the surface by NO, which ends up dominating the surface coverage and further

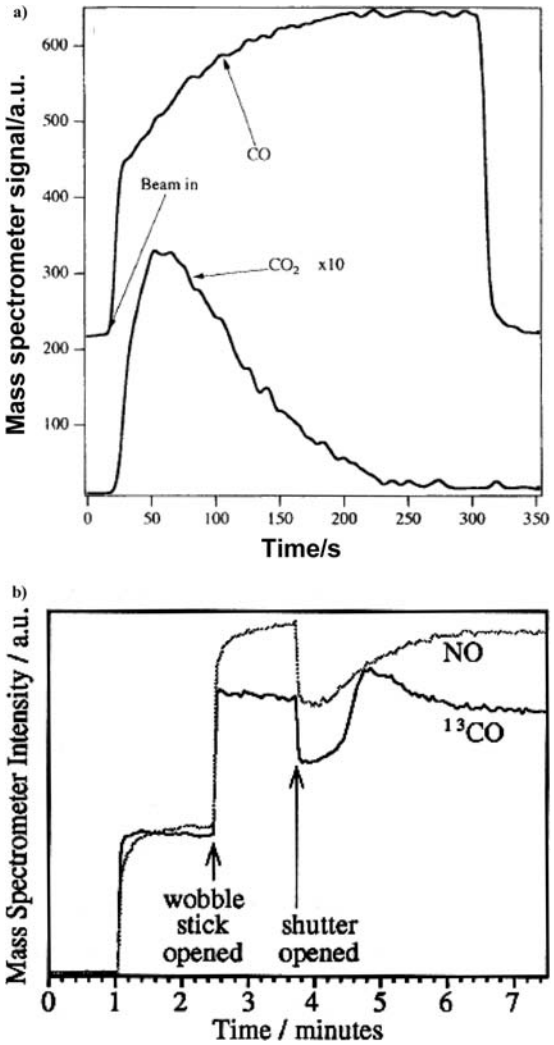

Fig. 5 Molecular beam experiments highlighting the differences in behaviour of Rh(110) and Pd(110) for reaction between CO and NO. In (a) CO in the beam reacts with a pre-adsorbed layer of NO on Rh(110), and instantaneous CO_2 production proves that NO has dissociated. In contrast, for Pd(110) (b), when a beam of CO and NO are introduced together onto the surface, both adsorb very efficiently (the pressure drop at 3.8 min when the beam is allowed to hit the surface), but no CO_2 is produced due to the inability of the Pd surface to dissociate NO at 300 K. It is also notable that CO is displaced from the surface after a little while (at ~5 min) by more strongly adsorbed NO.

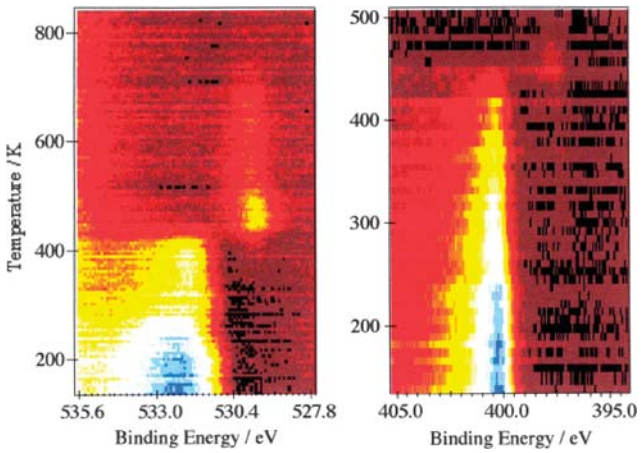

Fig. 6 TPXPS showing the dissociation of molecular NO on Pd(110) during heating.[18] The transition from molecularly adsorbed NO (binding energies 400 eV and 532.5 eV) to the dissociated state (binding energy for atomic oxygen 530 eV) occurs at about 420 K; note that N is lost to the gas phase upon dissociation of molecular NO as N_2O and N_2.[39]

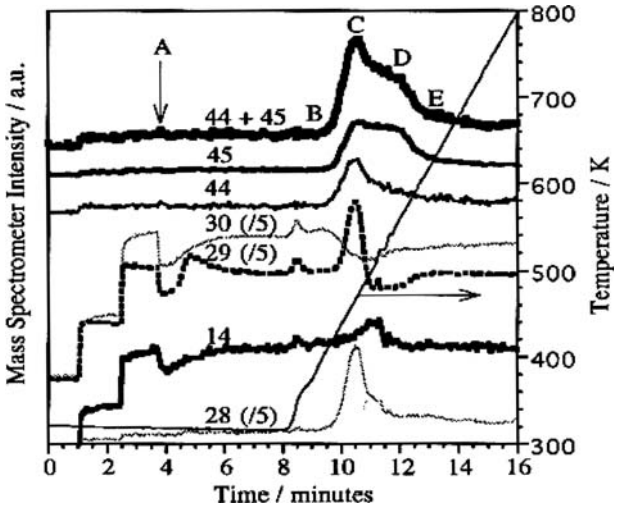

Fig. 7 A molecular beam experiment for the adsorption and temperature-programmed reaction between NO and labelled ^{13}CO on Pd(110).[18] The adsorption stage at A is similar to that in Fig. 5b, showing only molecular adsorption of NO and CO, with displacement of CO from the surface at about 5 min. However, evidence of NO dissociation is seen at 10 minutes (point B), during the heating sequence. Here carbon dioxide, nitrogen and nitrous oxide are all seen to evolve, reaching peak rate at point C.

implies a stronger binding of NO to the surface than CO. As can be seen in Fig. 6, using time-resolved and temperature-programmed XPS (TPXPS), dissociated states of NO are seen only above ~430 K after exposing the surface to NO and then heating it in a vacuum.[18] As a result no reaction occurs when CO is introduced to the surface at low temperature and shows that an essential requirement for this reaction is prior dissociation of the NO. However, even on Pd the reaction proceeds reasonably well if the surface is heated, as shown in molecular beam experiments, Fig. 7.[18,36,37] This is also reflected in TPXPS of the reaction, Fig. 8.[18,37] Here it is clear that, at first, CO adsorbs with NO (C(1s) binding energy at ~286 eV) at point A on the figure, but it is NO which outcompetes CO for surface sites (as also shown again by CO displacement from the surface at 5 min in Fig. 7), and so dominates the surface above 350 K (point B). At ~440 K NO desorption begins, which opens up sites for NO dissociation (point C); evidence for this in Fig. 6 and 8 is the appearance of the O(1s) signal at about 530 eV binding energy due to atomic oxygen, after heating to ~430 K and higher. This is the light-off point for this reaction, and is again due to a positive feedback due to the following overall reaction, which produces new, free sites:

$$2NO_a + 2CO_g + 2S \rightarrow N_{2g} + 2CO_{2g} + 4S \qquad (3)$$

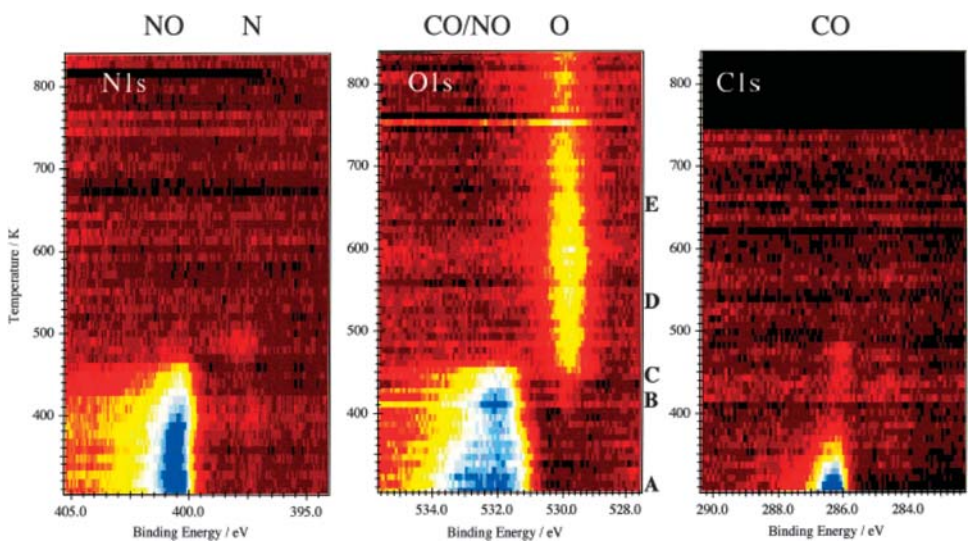

Fig. 8 The CO–NO reaction observed using TPXPS. Upon initial exposure of the Pd(110) surface to the mixture both CO (286 eV binding energy) and NO (400 eV binding energy) adsorb (point A), but CO is quickly displaced from the surface and is replaced by NO (point B). At point C the light-off of the CO–NO reaction begins as NO begins to desorb and dissociate. After this the surface is dominated by adsorbed atomic oxygen (530 eV binding energy).

As for eqn (2) above these can be broken down to elementary steps as follows:

$$2CO_g + 2S \rightarrow 2CO_a$$

$$2CO_a + 2NO_a \rightarrow N_{2g} + 2CO_{2g} + 4S$$

It must be noted that similar considerations apply for this reaction at higher pressures,[38] though there may also be other kinds of surface intermediates involved in the reaction, particularly the isocyanate species identified in IR measurements.

The rate of such reactions is strongly affected by adsorbate–adsorbate interactions which decrease their strength of adsorption as the coverage increases, and usually make the reaction easier. Adsorbate–adsorbate interactions have very significant effects on the stability of adsorbed molecules and atoms. It is particularly important for the oxygen, where strong interactions reduce the heat of adsorption on Pt single crystals from $\sim$350 kJ mol^{-1} at low coverage to $\sim$140 kJ mol^{-1} at high coverage.[39,40] An example of this is the adsorption on NO on Rh(110). Fig. 9a presents TPD results after the adsorption of NO, while molecular beam data are shown in Fig. 9b. The TPD shows clearly that the N atoms from NO dissociation are strongly held on Rh at low coverage (peak temperature of 550 K), but desorb much easier at high coverage (peak at 420 K), due to much weaker binding to the surface at high coverage,[41] largely because of repulsive interactions with the oxygen atoms that are left. Thus, in the molecular beam experiment of Fig. 9b, as NO adsorbs, so there is a delay until N_2 evolves into the gas phase. This is due to the decreasing heat of adsorption as increasing amounts of nitrogen atoms and oxygen atoms are deposited onto the surface, and hence the easier desorption of N_2. In the highest temperature molecular beam experiment the situation is a little more complicated. This temperature (576 K) is clearly in the range of desorption of the strongly-held state in Fig. 9a and so nitrogen desorption begins immediately. It then starts to reduce because the sticking probability for NO decreases as the coverage increases. However, at some point the coverage of oxygen and nitrogen atoms goes above a certain critical level (probably half of a monolayer of atoms) and the nitrogen atoms are suddenly destabilised (into the state shown in Fig. 9a, desorbing at 420 K), and so the rate of nitrogen evolution increases again before finally stopping once all the dissociative adsorption sites have been blocked by atomic oxygen. Obviously then, in the exhaust situation nitrogen will evolve significantly more quickly when the surface coverage is high, though NO dissociation itself will be impeded at saturation oxygen coverage.

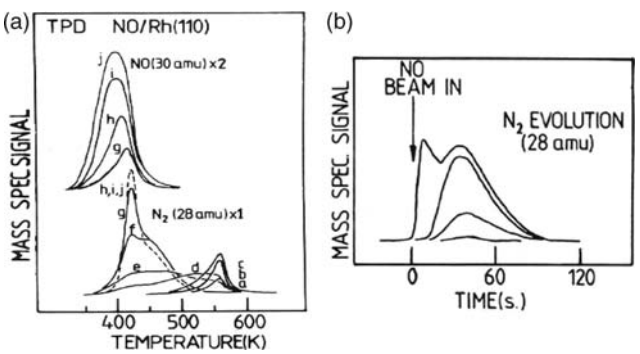

Fig. 9 (a) TPD after NO adsorption on Rh(110) for several different coverages. The coverages were (a) 0.3 L, (b) 0.6 L, (c) 1.5 L, (d) 1.8 L, (e) 2.1 L, (f) 3 L, (g) 4.2 L, (h) 5 L, (i) 6 L, (j) 12 L. As the coverage increases, so there is a critical decrease in the desorption energy of N_2 due to strong interactions with co-adsorbed oxygen atoms; (b) isothermal nitrogen desorption from Rh(110) observed while beaming NO onto the surface at several different crystal temperatures; in order of increasing nitrogen evolution they are 380, 411, 470 and 576 K.

4 Lean-burn engines, NO_x storage and reduction

As described in Section 1 above, Ba is now incorporated into some exhaust catalyst systems for use in NSR—so-called 'NO_x storage and reduction' catalysis. Surface science can have a significant impact on this relatively new area of science, particularly with respect to the mechanism of the reactions involved at the molecular scale and to the nature of the interaction between the active metal phase and the barium compound in the process. In recent studies we have looked at this system using what has been called the 'inverse catalyst' approach.[42,43] Here we use Pt(111) as a base on which to dose BaO to investigate the NO_x storage phenomenon. As shown in Fig. 10 it is possible to make a variety of structures of BaO in this way. Fig. 10a is an STM image of a relatively low coverage

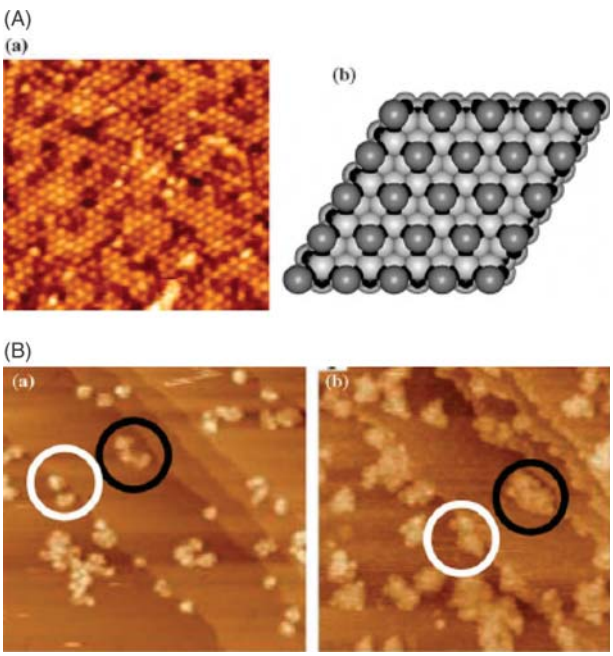

Fig. 10 (A) STM images of model catalysts of BaO on Pt(111). (a) A thin layer BaO film showing the (2 × 2) reconstruction (24.8 × 24.8 nm image size); (b) is a ball model of that surface. Dark spheres are surface Ba, light spheres are Ba atoms below the surface layer and black spheres are oxygen atoms.[43] (B) A higher coverage of BaO, showing additional nanoparticles of BaO; (a) is the as-prepared surface whereas (b) is after treatment in an equimolar NO and O_2 mixture (dosed into the chamber from separate lines) at 573 K and 3 × 10^{-7} mbar pressure. The particles have expanded due to the formation of nitrate, which has a much higher unit cell volume. Image sizes 90 × 90 nm. The circles highlight the same particles in the images before and after reaction.

of BaO on the surface, and shows that such layers are reconstructed in a (2 × 2) fashion.[44,45] In the unreconstructed state BaO(111) is a polar surface and is therefore theoretically unstable due to excess surface charge. The (2 × 2) reconstruction lowers the surface energy of the system by, crudely, equalising the cation/anion distribution at the surface (Tasker's rules[46]), lowering the excess charge and surface energy. Effectively, the (2 × 2) produces facets of (100) surface which has equal numbers of Ba^{2+} and O^{2-} ions[45] and has the lowest surface energy of all the low index faces. At multilayer coverages of BaO, particulate surfaces are produced, as shown in Fig. 10b. Important questions in respect of this system prevail in the catalytic literature, and these include:

(i) Is it NO or NO_2 that is necessary in the gas phase for storage to occur?

(ii) How does storage occur—just at the surface of the Ba particles, or throughout the bulk?

(iii) Does the storage occur only at places where BaO and precious metal are in contact?

The results of Fig. 10b clearly answer points (i) and (ii). Here the surface has been exposed to NO and O_2 (from separate dose sources) and clearly shows storage without the presence of NO_2 in the gas phase (although *surface* NO_2 may well be produced at Pt sites), while the degree of expansion of the BaO particles at the surface shows that the NO_x storage is not confined merely to the surface layer. Regarding (iii) above there is no doubt that the stored nitrate is catalytically decomposed by Pt in a solid state, homogeneous manner.[47]

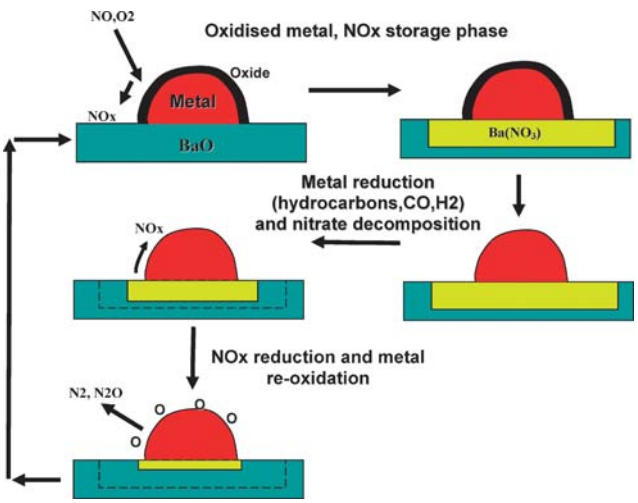

Fig. 11 A schematic, showing the various steps of the NSR process. Top left is the catalyst just into the oxidation phase of the exhaust cycle; in this stage NO_x in the exhaust can become stored on the barium component. Top right the Ba component is converted to nitrate and is saturated, so NO_x would appear in the exhaust stream unconverted. However, before that point (middle right panel) a slug of reductant (usually fuel) is injected into the exhaust system, providing a reducing environment with little oxygen present, so the surface oxide layer on the metal component is removed. At this point (middle left), the system is active for the decomposition of the adjacent Ba nitrate, and the released NO_x is reduced on the metal surface to produce nitrogen (bottom left); as this proceeds, the slug of reductant is no longer present, and so the cycle is completed and the surface becomes fully oxidised again.

This was proven by experiments with Pt impregnated barium nitrate[47] and with high surface area catalysts[47,48] for which the nitrate is decomposed at ~650 K, whereas in the absence of Pt the decomposition does not begin until above 750 K.

From such experiments a model of the NO_x storage and reduction process can be presented as shown in Fig. 11. Here the process is shown in several stages, involving oxidation of the precious metal component under normal lean-burn (oxygen rich) conditions, during which NO_x is not converted (due to the inactivity of the oxidised metal surface), but is instead stored on the Ba component as the nitrate. At a point close to the saturation of this nitrate layer, but before a significant amount of NO_x is released through the catalyst system, fuel-rich conditions are applied for a very short time, which reduces the metal component, which in turn then catalyses the decomposition of adjacent barium nitrate, and reduces the released NO_x to yield N_2 (and usually some N_2O too). After the reductant has passed through, the surface then gradually re-oxidises again, thus closing the cycle. In such catalysis the main role of Pt is to facilitate oxidation (including possible NO conversion to NO_2), while Rh is mainly there for NO_x reduction.

5 Conclusions

Surface science has had a significant impact on our understanding of catalytic phenomena associated with automotive depollution catalysis.

In oxidation reactions it has generally been found that reactions are self-poisoned at low temperatures by the presence of strongly adsorbed reactants (such as molecular CO), and that the rapid acceleration in rate at elevated temperatures (often called 'light-off') is due to the desorption of such adsorbates, which then frees up sites for oxygen dissociation and hence for oxidation reactions. Such autocatalytic phenomena can then manifest themselves as oscillatory reactions which can vary in surface reactant concentration and rate in both space and time.

For NO reduction, the efficiency of depollution (by production of molecular nitrogen) is strongly affected by the nature of the metal used. Rh is extremely effective because it can dissociate NO much more readily than metals such as Pd and Pt, enabling oxygen removal (by reaction with CO to CO_2 for instance) even at room temperature. Rh is also very selective in producing predominantly N_2, rather than N_2O.

NSR is an important development in removal of NO_x under the highly oxidising conditions of a lean-burn engine exhaust, and the strategy involves storing NO_x on BaO under oxidising conditions followed by the creation of reducing conditions to de-store and reduce it to nitrogen. By the use of STM it has been shown that this storage process is extremely facile, occurring fast even under UHV conditions, and that the storage occurs on BaO in the vicinity of Pt(111), with most of the oxide being converted to nitrate. The main effect of the reduction phase is to convert the oxidised metal surface, which is relatively unreactive, to the reduced surface, which can then both accelerate the decomposition of the nitrate phase in a homogeneous catalytic, solid state manner, and can reduce the NO/NO_2 so-produced at the surface.

References

1 K. C. Taylor, in *Catalysis: Science and Technology*, ed. J. R. Anderson and M. Boudart, Springer-Verlag, Berlin, 1984, vol. 5, p. 119.
2 H. S. Gandhi, G. W. Graham and R. W. McCabe, *J. Catal.*, 2003, **216**, 433.
3 K. C. Taylor, *Catal. Rev. Sci. Eng.*, 1993, **35**, 457.
4 M. V. Twigg, *Appl. Catal., B*, 2007, **70**, 2.
5 N. Takahashi, H. Shinjoh, T. Iijima, T. Suzuki, K. Yamazaki, K. Yokota, H. Suzuki, N. Miyoshi, S. Matsumoto, T. Tanizawa, T. Tanaka, S. Tateishi and K. Kasahara, *Catal. Today*, 1996, **27**, 63.
6 N. Miyoshi and S. Matsumoto, *Stud. Surf. Sci. Catal.*, 1999, **121**, 245.
7 S. Matsumoto, *CATTECH*, 2000, **4**, 102.
8 M. Takeuchi and S. Matsumoto, *Top. Catal.*, 2004, **28**, 151.
9 L. Gill, P. Blakeman, M. V. Twigg and A. P. Walker, *Top. Catal.*, 2004, **28**, 157.
10 T. Engel and G. Ertl, *Adv. Catal.*, 1979, **28**, 1.
11 G. Ertl and J. Koch, in *Proceedings of the 5th International Congress on Catalysis, Miami Beach (FL) 1972*, ed. J. W. Hightower, North Holland Publ. Co., Amsterdam, 1973, pp. 969–979.
12 T. Engel and G. Ertl, in *Proceedings of the 7th International Vacuum Congress and the 3rd International Conference on Solid Surfaces, Vienna, 1977*, ed. R. Dobrozemsky, F. Rüdenaver, F. P. Viehböck and A. Breth, F. Berger & Söhne, Vienna, 1977, pp. 1365–1368.
13 T. Engel and G. Ertl, *Chem. Phys. Lett.*, 1978, **54**, 95.
14 T. Engel and G. Ertl, *J. Chem. Phys.*, 1978, **69**, 1267.
15 M. Bowker, *The Basis and Applications of Heterogeneous Catalysis*, Oxford Chemistry Primers, OUP, Oxford, UK, 1998.
16 J. M. Thomas and W. J. Thomas, *Principles and Practice of Heterogeneous Catalysis*, VCH, Weinheim, 1997.
17 I. Z. Jones, R. A. Bennett and M. Bowker, *Surf. Sci.*, 1999, **439**, 235.
18 I. Z. Jones, *PhD Thesis*, University of Reading, Reading, 1999.
19 For a review of some of this work, see: G. Ertl, *Faraday Discuss.*, 2002, **121**, 1.
20 G. Ertl, P. R. Norton and J. Rüstig, *Phys. Rev. Lett.*, 1982, **49**, 177.
21 J. Jakubith, H. Rotermund, W. Engel, A. von Oertzen and G. Ertl, *Phys. Rev. Lett.*, 1990, **65**, 3013.
22 G. Ertl, *Adv. Catal.*, 2000, **45**, 1.
23 M. Bertram, C. Beta, H. H. Rotermund and G. Ertl, *J. Phys. Chem. B*, 2003, **107**, 9610.
24 M. Bertram, C. Beta, M. Pollmann, A. S. Mikhailov, H. H. Rotermund and G. Ertl, *Phys. Rev. E: Stat. Phys., Plasmas, Fluids, Relat. Interdiscip. Top.*, 2003, **67**, 036208-1-9.
25 http://nobelprize.org/nobel_prizes/chemistry/laureates/2007/index.html.
26 A. W. Santra and D. W. Goodman, *Electrochim. Acta*, 2002, **47**, 3595.
27 J. C. Campuzano, in *The Chemical Physics of Solid Surfaces and Heterogeneous Catalysis*, ed. D. A. King and D. P. Woodruff, Elsevier, Amsterdam, 1990, vol. 3, pp. 389–460.
28 M. Haruta, T. Kobayashi, H. Sano and Y. N, *Chem. Lett.*, 1987, 405.
29 M. Haruta, S. Tsubota, T. Kobayashi, H. Kageyama, M. J. Genet and B. Delmont, *J. Catal.*, 1993, **144**, 175.
30 G. C. Bond and D. T. Thompson, *Catal. Rev. Sci. Eng.*, 1999, **41**, 319.
31 M. Bowker, A. Nuhu and J. Soares, *Catal. Today*, 2007, **122**, 245.
32 See, for instance: V. Gorodetskii, W. Drachsel and J. H. Block, *J. Chem. Phys.*, 1994, **100**, 6915.
33 See, for instance: H. Wei, G. Lilienkamp and R. Imbihl, *Chem. Phys. Lett.*, 2001, **336**, 181.
34 See, for instance: *Oscillations and Travelling Waves in Chemical Systems*, ed. R. J. Field and M. Burger, Wiley, NY, 1985.
35 M. Bowker, Q. Guo, Y. Li and R. W. Joyner, *J. Chem. Soc., Faraday Trans.*, 1995, **91**, 3663.
36 R. Sharpe and M. Bowker, *Surf. Sci.*, 1996, **360**, 21.
37 M. Bowker and R. A. Bennett, *Top. Catal.*, 2004, **28**, 25.
38 E. Osenzoy, C. Hess and D. W. Goodman, *Top. Catal.*, 2004, **28**, 13.
39 C. Wartnaby, A. Stuck, Y. Yeo and D. A. King, *J. Phys. Chem.*, 1996, **100**, 12483.
40 Y. Yeo, L. Vattuone and D. A. King, *J. Chem. Phys.*, 1997, **106**, 392.
41 M. Bowker, Q. Guo and R. W. Joyner, *Surf. Sci.*, 1991, **257**, 33.
42 H.-J. Freund, M. Baumer and H. Kuhlenbeck, *Adv. Catal.*, 2000, **45**, 333.
43 J. Libuda and H.-J. Freund, *Surf. Sci. Rep.*, 2005, **57**, 157.
44 P. Stone, M. Ishii and M. Bowker, *Surf. Sci.*, 2003, **537**, 179.
45 M. Bowker, P. Stone, R. Smith, E. Fourre, M. Ishii and N. H. de Leeuw, *Surf. Sci.*, 2006, **600**, 1973.
46 P. W. Tasker, *Philos. Mag. A*, 1979, **39**, 119.
47 D. James, E. Fourre, M. Ishii and M. Bowker, *Appl. Catal., B*, 2003, **45**, 147.
48 S. Poulston and R. Rajaram, *Catal. Today*, 2003, **81**, 603.